Increased Amazon Basin wet-season precipitation and river discharge since the early 1990s driven by tropical Pacific variability

Andrew R. Friedman, Massimo Bollasina, Guillaume Gastineau, Myriam Khodri

ENVIRONMENTAL RESEARCH
LETTERS

LETTER • OPEN ACCESS

Increased Amazon Basin wet-season precipitation and river discharge since the early 1990s driven by tropical Pacific variability

IOP Publishing Environ. Res. Lett. 16 (2021) 034033 https://doi.org/10.1088/1748-9326/abd587

ENVIRONMENTAL RESEARCH
LETTERS

OPEN ACCESS

RECEIVED
3 July 2020

REVISED
25 November 2020

ACCEPTED FOR PUBLICATION
21 December 2020

PUBLISHED
25 February 2021

LETTER

Increased Amazon Basin wet-season precipitation and river discharge since the early 1990s driven by tropical Pacific variability

Andrew R Friedman[1,2,*], **Massimo A Bollasina**[1], **Guillaume Gastineau**[3] and **Myriam Khodri**[3]

[1] School of Geosciences, University of Edinburgh, Edinburgh, United Kingdom
[2] Institute of Geography and Oeschger Centre for Climate Change Research, University of Bern, Bern, Switzerland
[3] UMR LOCEAN, Sorbonne Université/IRD/MNHN/CNRS, Paris, France
[*] Author to whom any correspondence should be addressed.

E-mail: andrew.friedman@giub.unibe.ch

Keywords: Walker circulation, Pacific decadal variability, Amazon River discharge, wind stress forcing, Amazon Basin precipitation, large ensemble simulations

Supplementary material for this article is available online

Abstract

The Amazon Basin, the largest watershed on Earth, experienced a significant increase in wet-season precipitation and high-season river discharge from the early 1990s to early 2010s. Some studies have linked the increased Amazon Basin hydrologic cycle to decadal trends of increased Pacific trade winds, eastern Pacific sea surface temperature (SST) cooling, and associated strengthening of the Pacific Walker circulation. However, it has been difficult to disentangle the role of Pacific decadal variability from the impacts of greenhouse gases and other external climate drivers over the same period. Here, we separate the contributions of external forcings from those of Pacific decadal variability by comparing two large ensembles of climate model experiments with identical radiative forcing agents but imposing different tropical Pacific wind stress. One ensemble constrains tropical Pacific wind stress to its long-term climatology, suppressing tropical Pacific decadal variability; the other ensemble imposes the observed tropical Pacific wind stress anomalies, simulating realistic tropical Pacific decadal variability. Comparing the Amazon Basin hydroclimate response in the two ensembles allows us to distinguish the contributions of external forcings common to both simulations from those related to Pacific trade wind variability. For the 1992–2012 trend, the experiments with observed tropical Pacific wind stress anomalies simulate strengthening of the Walker circulation between the Pacific and South America and sharpening of the Pacific–Atlantic interbasin SST contrast, driving increased Amazon Basin wet-season precipitation and high-season discharge. In contrast, these circulation and hydrologic intensification trends are absent in the simulations with climatological tropical Pacific wind stress. This work underscores the importance of Pacific decadal variability in driving hydrological cycle changes and modulating the hydroclimate impacts of global warming over the Amazon Basin.

1. Introduction

The Amazon River is by far the Earth's largest river by flow, responsible for 15%–20% of the freshwater discharged into the oceans (Molinier *et al* 1996, Dai *et al* 2009). Its basin holds the largest planetary watershed and rainforest, which play key roles in the global climate system and carbon cycle and contain a wealth of biodiversity (Foley *et al* 2002, Malhi *et al* 2008). Recent extensive Amazon Basin dry-season droughts and fires have heightened concerns about climate change and deforestation (Nobre *et al* 2016, Marengo *et al* 2018). Additionally, starting in the early 1990s, the Amazon Basin experienced a dramatic increase in wet-season (December–May) precipitation, resulting in a strengthening of the hydrological cycle, heightened peak river discharge, and disruptive flood events (Gloor *et al* 2013, 2015, Marengo and Espinoza 2016, Barichivich *et al* 2018). The increased river discharge also reduced tropical Atlantic surface salinity

(Gouveia *et al* 2019), with potential impacts on ocean circulation and large-scale climate (Jahfer *et al* 2017). Understanding the causes of this recent Amazon Basin hydrological intensification is important for assessing the uncertainties associated with climate change projections.

The Amazon Basin hydrological cycle intensification coincided with a pronounced climatic shift in the tropical Pacific. Over the 20-year period beginning in the early 1990s, the Pacific trade winds experienced a strengthening which was unprecedented within instrumental and reanalysis records (Balmaseda *et al* 2013, de Boisséson *et al* 2014). This was associated with sea surface temperature (SST) cooling in the equatorial central and eastern Pacific, and a reduced rate of global surface temperature increase compared to previous decades, sometimes referred to as the *hiatus* (Meehl *et al* 2011, Kosaka and Xie 2013). The trade wind and SST changes were connected to a strengthening of the Pacific Walker circulation and more frequent La Niña phases of the El Niño/-Southern Oscillation (ENSO) (Dong and Lu 2013, Liu and Zhou 2017). On decadal timescales, these trends reflected a transition from the warm to cold phases of the Interdecadal Pacific Oscillation (IPO; Zhang *et al* 1997, Power *et al* 1999), with a larger amplitude than previous transitions (England *et al* 2014).

Observational analysis has connected the Amazon Basin wet-season precipitation increase from the early 1990s to the Pacific trade wind strengthening, SST cooling, and intensified Walker circulation (Barichivich *et al* 2018), building on well-established ENSO teleconnections in the tropics (Ropelewski and Halpert 1987, Dai and Wigley 2000). However, it is difficult using observations alone to separate the influence of Pacific variability on Amazon precipitation from that of greenhouse gases (GHGs) and other external climate forcing agents over the same period. As such, climate model sensitivity experiments can be useful to differentiate the contemporaneous impacts of different drivers (Hegerl and Zwiers 2011).

In this study, we use a set of companion large-ensemble climate model simulations with tropical Pacific surface wind stress nudging. The two experiments have identical external forcing agents but impose different wind stress regimes in the tropical Pacific, while allowing the climate system to evolve freely outside the tropical Pacific. In the first ensemble, W-CLIM, tropical Pacific wind stress is constrained to its long-term climatology, simulating the counterfactual trajectory of the climate system holding a fixed neutral IPO state. In the second ensemble, W-FULL, observed tropical Pacific wind stress anomalies are imposed, simulating the evolution of the climate system with realistic tropical Pacific decadal variability, including the trade wind acceleration from the early 1990s and IPO phase transition. By comparing the Amazon Basin hydroclimate response in W-CLIM and W-FULL, we can distinguish the contributions of the external forcings common to both simulations from those related to Pacific trade wind variability found only in W-FULL.

2. Methods and data

We examine a set of experiments with the IPSL-CM5A-LR global climate model (Dufresne *et al* 2013). Its atmospheric component is LMDZ5A (Hourdin *et al* 2013), with a resolution of 3.75° × 1.875° and 39 vertical levels. The land surface component is ORCHIDEE (Krinner *et al* 2005), with a similar horizontal resolution as the atmosphere, and the ocean component is NEMOv3.2 (Madec 2008). The experimental setup, further described in Gastineau *et al* (2019), consists of two 30-member ensembles, each initialized in 1979 from a spread of random phases of the IPO and the Atlantic Multidecadal Oscillation (AMO) (Kerr 2000) from the IPSL-CM5A-LR fully-coupled historical large ensemble (Frankignoul *et al* 2017). Both ensembles are forced by identical Fifth Coupled Model Intercomparison Project (CMIP5) historical and Representative Concentration Pathway 8.5 (RCP8.5) GHG and ozone emissions from 1979 to 2014 (Taylor *et al* 2012). Volcanic aerosols are included, but anthropogenic aerosols are fixed at 1940 values in both experiments.

In both ensembles, wind stress (τ) is prescribed in the ocean component in the tropical Pacific from 20° S to 20° N with a buffer region from 15° to 25° latitude (outlined in figure 1(a)), while leaving the climate system unconstrained outside the tropical Pacific. Prescribing wind stress tightly constrains SST through its effects on zonal advection, thermocline depth, and eastern Pacific upwelling (Clarke 2008). It is somewhat similar to nudging SST (e.g. Kosaka and Xie 2013, McGregor *et al* 2014), but favors the dynamical consistency between the atmosphere and ocean, and reduces artificial heat fluxes imposed into the ocean (Watanabe *et al* 2014, Douville *et al* 2015). In the representative climatological ensemble, W-CLIM, the 1979–2014 climatological wind stress from the IPSL-CM5A-LR historical and RCP8.5 CMIP5 ensemble mean is prescribed, with additional model noise to deepen the mixed layer; this is further described in text S1 (which is available online at stacks.iop.org/ERL/16/034033/mmedia).

In the second ensemble, W-FULL, daily wind stress anomalies from 1979 to 2014 from the ECMWF ERA-Interim Reanalysis (ERA-I; Dee *et al* 2011) are added to the model climatology and prescribed in the ocean model component. Figure 1(a) shows the 1992–2012 ERA-I mean τ trend over the nudging region during the Amazon Basin wet season (December–May). Figure 1(b) shows the corresponding zonal wind stress (τ_x) anomaly over the Niño 4 region (160° E–150° W, 6° S–6° N) from ERA-I

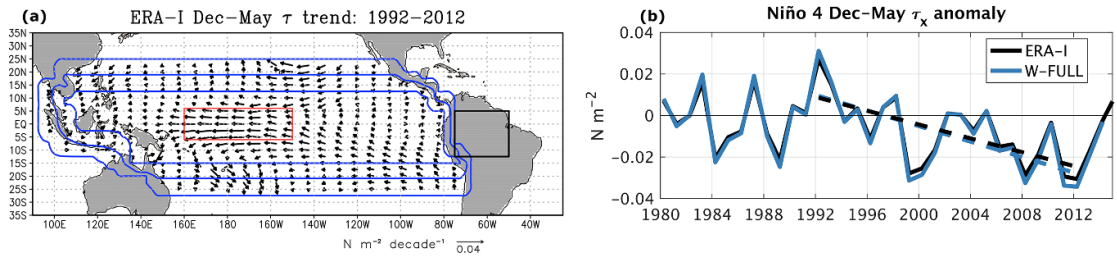

Figure 1. Pacific wind stress nudging mask and trend. (a) 1992–2012 December–May mean ERA-I wind stress (τ) trend over the nudging mask region, in N m^{-2} decade^{-1}. Blue contour intervals indicate regions of 0%, 50%, and 100% blending of model and nudged τ. The red box outlines the Niño 4 region (160° E–150° W, 6° S–6° N) and the black box outlines the Amazon precipitation region. (b) December–May mean zonal wind stress (τ_x) anomaly over Niño 4 from ERA-I and applied in W-FULL, in N m^{-2}. Anomalies are computed from the 1980–1992 climatology; dashed lines indicate the 1992–2012 trend.

and applied in W-FULL, illustrating the significant ($p < 0.05$) strengthening trend from 1992 to 2012. An error in the treatment of the ERA-I τ anomalies induced τ amplitudes about 20% larger in W-FULL than ERA-I, though the overall interannual changes are very similar and the spatial patterns are identical (Gastineau *et al* 2020).

For precipitation, we examine the monthly 2.5° × 2.5° combined satellite-gauge Global Precipitation Climatology Project (GPCP), version 2.3 (Adler *et al* 2003, 2018). We take December–May as the Amazon Basin-wide wet season, which is associated with the South American monsoon system, while recognizing that the seasonal cycle varies regionally within the Basin (Marengo *et al* 2012, Wang *et al* 2018). IPSL-CM5A-LR generally reproduces the observed wet-season regional precipitation climatology (figures S1(a)–(c)). In common with many CMIP5 models, it suffers from a double intertropical convergence zone (ITCZ) in the eastern Pacific (Jones and Carvalho 2013, Li and Xie 2014). There is also excessive precipitation over the Andes relative to the Amazon Basin interior (Dufresne *et al* 2013). IPSL-CM5A-LR effectively simulates the observed seasonal cycle of Amazon region mean precipitation (figure S1(d)), though similar to many CMIP5 models, it underestimates total precipitation, particularly during the July–October dry season (Yin *et al* 2013).

To complement precipitation, we examine monthly Amazon River discharge (in m^3 s^{-1}) from the farthest downstream long-term gauge at Óbidos (55.7° W, 1.9° S; indicated in figure 2(a)), which captures runoff from most of the Amazon Basin (Dai and Trenberth 2002). River discharge provides an integrated measure of Amazon Basin hydroclimate, though it does not allow us to differentiate between recirculated and non-recirculated precipitation (Gloor *et al* 2013, Dai 2016). For the model, we use the output of freshwater flux into the ocean from rivers (in kg m^{-2} s^{-1}) multiplied by the respective gridcell area to obtain a monthly volume flux, which we integrate over the Amazon River outflow region (45°–51° W, 2° S–6° N; blue box in figures 2(b)–(c)).

In observations, the Amazon River discharge climatology exhibits a relatively smooth seasonal cycle (figure S1(e)), gradually peaking in May and June. Óbidos discharge lags Basin-average precipitation by around 3 months due to the time for surface runoff to travel downstream (Dai and Trenberth 2002, Marengo 2005). The model seasonal discharge maximum arrives 1–2 months early, peaking in April, and lasts for a shorter period compared to observations, which reflects ORCHIDEE deficiencies over the Amazon region (Guimberteau *et al* 2012, 2014) and its floodplain storage not being activated in the CMIP5 experiments (Agnès Ducharne, personal communication). To allow for comparison between observations and simulations given the annual cycle phase differences, we track high-season discharge by taking the mean of the five largest-discharge months of each year (with the discharge year spanning from February to January). In addition to precipitation and discharge, we use the monthly 2° × 2° NOAA Extended Reconstructed SST dataset (ERSST), version 5 (Huang *et al* 2017), as well as monthly 2.5° × 2.5° atmospheric fields from ERA-I.

Our analysis focuses on the Amazon region wet season, for which the tropical Pacific has a relatively large influence on interannual variability (Yoon and Zeng 2010, Andreoli *et al* 2012), over the 21-year trend from 1992 to 2012, corresponding to the maximum Pacific trade wind strengthening (Balmaseda *et al* 2013, de Boisséson *et al* 2014). Trend significance is calculated based on a two-tailed Student's t-test of the slope, adjusting the standard error and degrees of freedom assuming a first-order autoregressive (AR1) noise model (Santer *et al* 2000). We also examine interannual correlations of linearly-detrended time series over the entire 1980–2014 period, with significance evaluated based on a two-tailed Student's t-test, adjusting the degrees of freedom assuming an AR1 noise model (Bretherton *et al* 1999). We describe trends and correlations as significant when $p < 0.05$. The W-CLIM and W-FULL ensemble means are analyzed in order to emphasize the robust signals in each experiment.

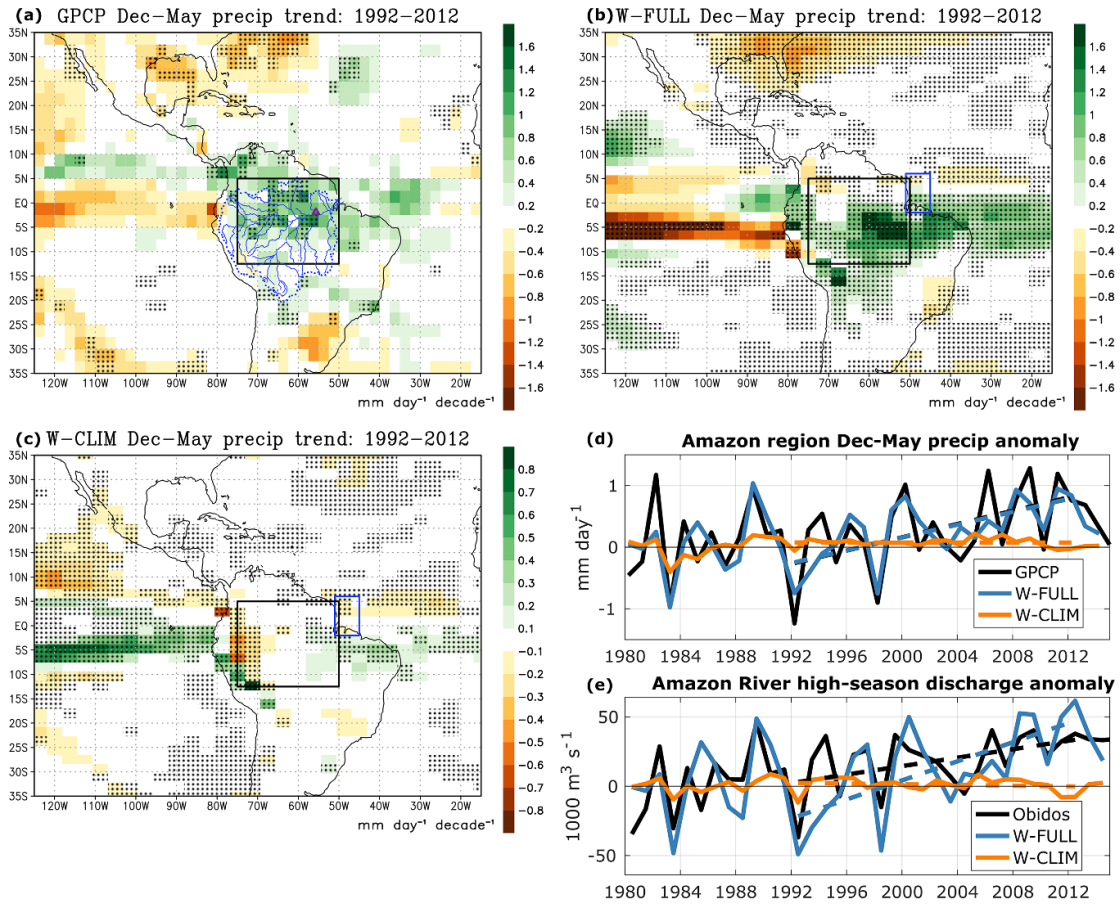

Figure 2. Wet-season precipitation and high-season river discharge. (a)–(c) 1992–2012 December–May mean precipitation trend, in mm d^{-1} $decade^{-1}$: (a) GPCP, (b) W-FULL, and (c) W-CLIM (note doubled color scale). Stippled regions are significant at $p < 0.05$. The black box outlines the Amazon precipitation region (75°–50° W, 12.5° S–5° N). In (a), the Amazon drainage basin and river system are indicated by the dotted black and solid blue lines respectively, and the triangle marks the Óbidos gauge station. In (b) and (c), the blue box indicates the region used to calculate Amazon River discharge. (d) December–May mean Amazon region precipitation anomaly for GPCP, W-FULL, and W-CLIM, in mm d^{-1}. (e) Mean high-season (5 largest months) Amazon River discharge anomaly from Óbidos, W-FULL, and W-CLIM, in 10^3 m^3 s^{-1}. Anomalies in (d) and (e) are computed from the 1980–1992 climatology; dashed lines indicate the 1992–2012 trend.

3. Results

3.1. Precipitation and discharge trends

The 1992–2012 observed wet-season precipitation trend (figure 2(a)) is positive over the Amazon Basin and northern South America extending into the equatorial Atlantic. In the eastern Pacific, it is positive from 5° to 10° N and negative along the equator. W-FULL (figure 2(b)) well reproduces the spatial pattern and magnitude of the observed trend, though the precipitation increase in South America is shifted to the south, with some drying in the northern Amazon region. W-FULL also overestimates the positive trend in the equatorial Atlantic and the negative trend in the eastern equatorial Pacific. W-CLIM (figure 2(c)), which has much smaller amplitudes (note doubled color scale), shows wettening in the eastern equatorial Pacific contrasting with drying in the western Amazon region, and a weaker precipitation increase in the eastern Amazon region extending into the equatorial Atlantic.

Figure 2(d) shows the observed and simulated wet-season mean precipitation anomaly averaged over the Amazon region (75°–50° W, 12.5° S–5° N) and 1992–2012 linear trend. W-FULL reproduces the significant positive 1992–2012 trend found in observations (table 1). It also captures much of the observed interannual variability, with a significant correlation with GPCP (table 2). The mean 5-month high-season Amazon River discharge is shown in figure 2(e). Like precipitation, W-FULL captures the 1992–2012 positive trend and is significantly correlated with Óbidos observations. W-CLIM lacks a discernible trend in basin-wide precipitation or river discharge.

3.2. SST and atmospheric circulation

The 1992–2012 trends in relative SST and low-level (850-hPa) wind are shown in figures 3(a)–(c). Relative SST (referred to as SST*), the deviation from the tropical mean (20° S–20° N) SST, captures the spatial gradients of SST and low-level moisture

Table 1. Wet-season trends. 1992–2012 trends for observations and W-FULL and W-CLIM ensemble means, in decade^{-1}; mean slope and 95% confidence intervals. Top: December–May mean Amazon region (75°–50° W, 12.5° S–5° N) precipitation. Middle: mean high-season (5 largest months) Amazon River discharge. Bottom: December–May mean Pacific–Atlantic interbasin SST contrast (tropical central and eastern Pacific (180°–90° W, 10° S–10° N) minus tropical Atlantic (40° W–15° E, 10° S–10° N) SST).

	Observations	W-FULL	W-CLIM
December–May Amazon region precipitation	0.54 ± 0.41 mm d^{-1} (GPCP)	0.52 ± 0.28 mm d^{-1}	-0.00 ± 0.06 mm d^{-1}
5-month max Amazon River discharge	$15.2 \pm 13.0 \times 10^3$ m^3 s^{-1} (Óbidos)	$34.4 \pm 18.3 \times 10^3$ m^3 s^{-1}	$-1.3 \pm 4.5 \times 10^3$ m^3 s^{-1}
December–May Pac–Atl ΔSST	-0.55 ± 0.37 °C (ERSST)	-0.75 ± 0.45 °C	0.03 ± 0.025 °C

Table 2. Wet-season interannual correlations. 1980–2014 detrended correlations of observations with W-FULL and W-CLIM ensemble means. Asterisks indicate statistically significant correlations at the 95% confidence level. Top: December–May mean Amazon region (75°–50° W, 12.5° S–5° N) precipitation. Middle: mean high-season (5 largest months) Amazon River discharge. Bottom: December–May mean Pacific–Atlantic interbasin SST contrast (tropical central and eastern Pacific (180°–90° W, 10° S–10° N) minus tropical Atlantic (40° W–15° E, 10° S–10° N) SST).

	W-FULL	W-CLIM
December–May Amazon region precipitation (GPCP)	0.72*	0.32
5-month max Amazon River discharge (Óbidos)	0.57*	0.41*
December–May Pac–Atl Δ SST (ERSST)	0.90*	0.05

which are important for tropical convection (Vecchi and Soden 2007, Ma and Xie 2013, Khodri *et al* 2017); absolute SST is shown in figures S2(a)–(c). ERSST (figure 3(a)) features SST* cooling in the tropical central and eastern Pacific resembling the pattern associated with the transition from positive to negative IPO phases, with equatorial SST* cooling extending into both hemispheres along the eastern boundary, and SST* warming in the tropical Atlantic. W-FULL (figure 3(b)) shows a similar pattern, though with larger-amplitude equatorial Pacific SST* cooling and without extending toward the mid-latitudes. These differences may reflect the larger-amplitude τ anomalies applied (Gastineau *et al* 2020) or model cold tongue SST and double ITCZ biases (Bellenger *et al* 2014, Li and Xie 2014). In contrast, W-CLIM (figure 3(c)) shows equatorial Pacific SST* warming, as expected from global warming processes found in coupled models (Dinezio *et al* 2009). ERA-I and W-FULL feature increased 850-hPa flow into the Amazon region from the tropical North Atlantic, one of the key pathways for Amazon climatological moisture convergence (Grimm 2003, Arraut *et al* 2012).

Figure 3(d) presents variations of the Pacific–Atlantic interbasin SST contrast (Pac–Atl ΔSST), which reflects the strength of the Walker circulation (Wang 2006, McGregor *et al* 2014, Chikamoto *et al* 2015) and has been linked to wet-season Amazon region precipitation (Gloor *et al* 2015, Barichivich *et al* 2018). Pac–Atl ΔSST is calculated as the difference between the tropical central and eastern Pacific (180°–90° W, 10° S–10° N) and the tropical Atlantic (40° W–15° E, 10° S–10° N; boxes in figures 3(a)–(c)). We find that Pac–Atl ΔSST is significantly negatively correlated with Amazon Basin wet-season precipitation and high-season river discharge in observations and the simulations (table S1). Consistent with the precipitation and discharge trends, W-FULL captures the significant 1992–2012 observed negative Pac–Atl ΔSST trend (table 1). The discrepancy between tropical North Atlantic SST* warming in ERSST compared to tropical South Atlantic SST* warming in W-FULL is not reflected in Pac–Atl △SST. In contrast, the W-CLIM Pac–Atl ΔSST trend is an order of magnitude smaller and of opposite sign.

In order to more clearly identify the zonal circulation changes, we examine the trends in pressure vertical velocity (ω) and the zonal component of the divergent wind (u_{div}) averaged over the maximum precipitation trend signal over the Amazon latitudes (0–10° S; figure 4). ERA-I and W-FULL feature increased ascent over the Amazon region and weakened ascent over the central equatorial Pacific (figures 4(a) and (b)), depicting strengthening of the climatological Walker circulation branch between the Pacific and South America (Dong and Lu 2013, Liu and Zhou 2017). In contrast, W-CLIM features a small weakening of the ascent over the western Amazon region (figure 4(c)), consistent with the weakening of the Walker circulation expected from global warming (Vecchi and Soden 2007). The meridional circulation, depicted through ω and the meridional component of the divergent wind (v_{div}) zonally averaged from 75° to 50° W (figure S3), also reveals enhanced Amazon uplift in ERA-I and W-FULL, though displaced to the south in W-FULL.

3.3. Moisture convergence

We next examine moisture convergence, which is the predominant contributor to Amazon Basin wet-season precipitation and the leading driver of its interannual variability (Angelini *et al* 2011, Satyamurty *et al* 2013b, Drumond *et al* 2014). ERA-I and the simulations feature climatological wet-season moisture convergence over the Amazon region (table

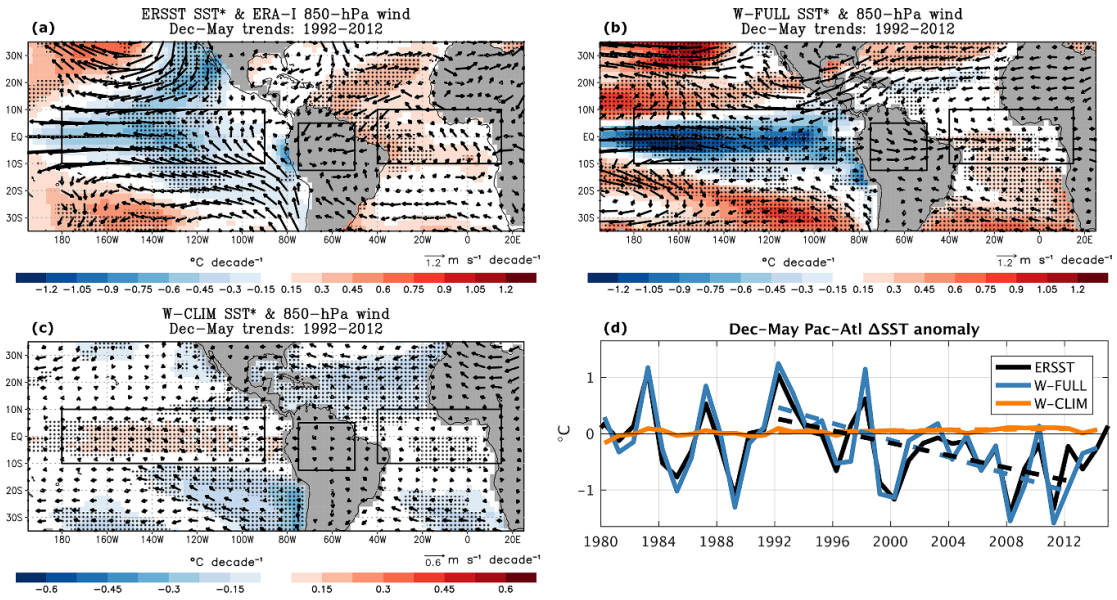

Figure 3. Relative SST, low-level wind, and interbasin SST contrast. (a)–(c) 1992–2012 December–May mean trend in relative SST (SST*, in °C decade^{-1}) and 850-hPa wind (in m s^{-1} decade^{-1}): (a) ERSST and ERA-I, (b) W-FULL, and (c) W-CLIM (note doubled color and wind scales). Stippled regions are significant at $p < 0.05$. Ocean boxes show the regions used to construct the Pacific–Atlantic interbasin SST contrast (Pac–Atl ΔSST): the tropical central and eastern Pacific (180°–90° W, 10° S–10° N) and tropical Atlantic (40° W–15° E, 10° S–10° N). (d) December–May mean Pac–Atl ΔSST anomaly, in °C. Anomalies in (d) are computed from the 1980–1992 climatology; dashed lines indicate the 1992–2012 trend.

S2(a) and figure S4). Consistent with the precipitation and discharge increases, ERA-I and W-FULL have significant positive moisture convergence trends over the Amazon region from 1992 to 2012 (table S2(b) and figure S5). Following Satyamurty *et al* (2013a, 2013b), we also integrate the moisture fluxes across the four Amazon region boundaries. Increased ERA-I moisture convergence is mostly due to northeasterly moisture advection from the tropical North Atlantic, while W-FULL simulates increased westerly moisture flux from the equatorial Pacific.

We additionally use the linear approximation of Huang (2014) to separate the moisture convergence components related to dynamics and thermodynamics in the 1992–2012 Amazon region trend:

$$\Delta P \sim \Delta\omega \cdot \bar{q} + \bar{\omega} \cdot \Delta q,$$

where P is precipitation; q denotes 925-hPa specific humidity; and ω is 500-hPa pressure velocity. The dynamic component ($\Delta\omega \cdot \bar{q}$) accounts for nearly all of the Amazon region moisture convergence increase in ERA-I and W-FULL, indicating that atmospheric circulation changes are predominant for the precipitation trend (table S3). In W-CLIM, which has little overall moisture convergence change, the increased thermodynamic component ($\bar{\omega} \cdot \Delta q$) opposes the reduced dynamic component related to the tropical circulation weakening.

4. Discussion

Using a companion set of climate model experiments with identical external forcing agents but differently constrained tropical Pacific wind stress, we attribute the 1992–2012 increases in wet-season Amazon Basin precipitation and high-season river discharge to the contemporaneous Pacific trade wind strengthening. In simulations with observed tropical Pacific wind stress anomalies (W-FULL), the imposed Pacific trades cause equatorial Pacific SST cooling, sharpening the Pacific–Atlantic zonal SST contrast (Pac–Atl ΔSST) and strengthening the Pacific-South America branch of the Walker circulation. The enhanced central and eastern Pacific subsidence and compensating convergence over the Amazon climatological ascending region lead to increased Amazon Basin wet-season precipitation and high-season river discharge (Gloor *et al* 2015, Barichivich *et al* 2018).

In contrast, the companion experiment with climatological tropical Pacific wind stress simulating a neutral IPO state (W-CLIM) does not produce significant changes in Amazon Basin wet-season precipitation or high-season river discharge. W-CLIM does have a larger 1992–2012 trend in absolute tropical Atlantic SST than W-FULL (figure S2(d)), though not in relative Pac–Atl ΔSST (figure 3(d)) which is important for Amazon Basin wet-season convection. While atmosphere-only experiments have shown a strong influence of Atlantic SST warming alone on the Amazon region wet-season precipitation increase from 1979 to 2015 (Wang *et al* 2018),

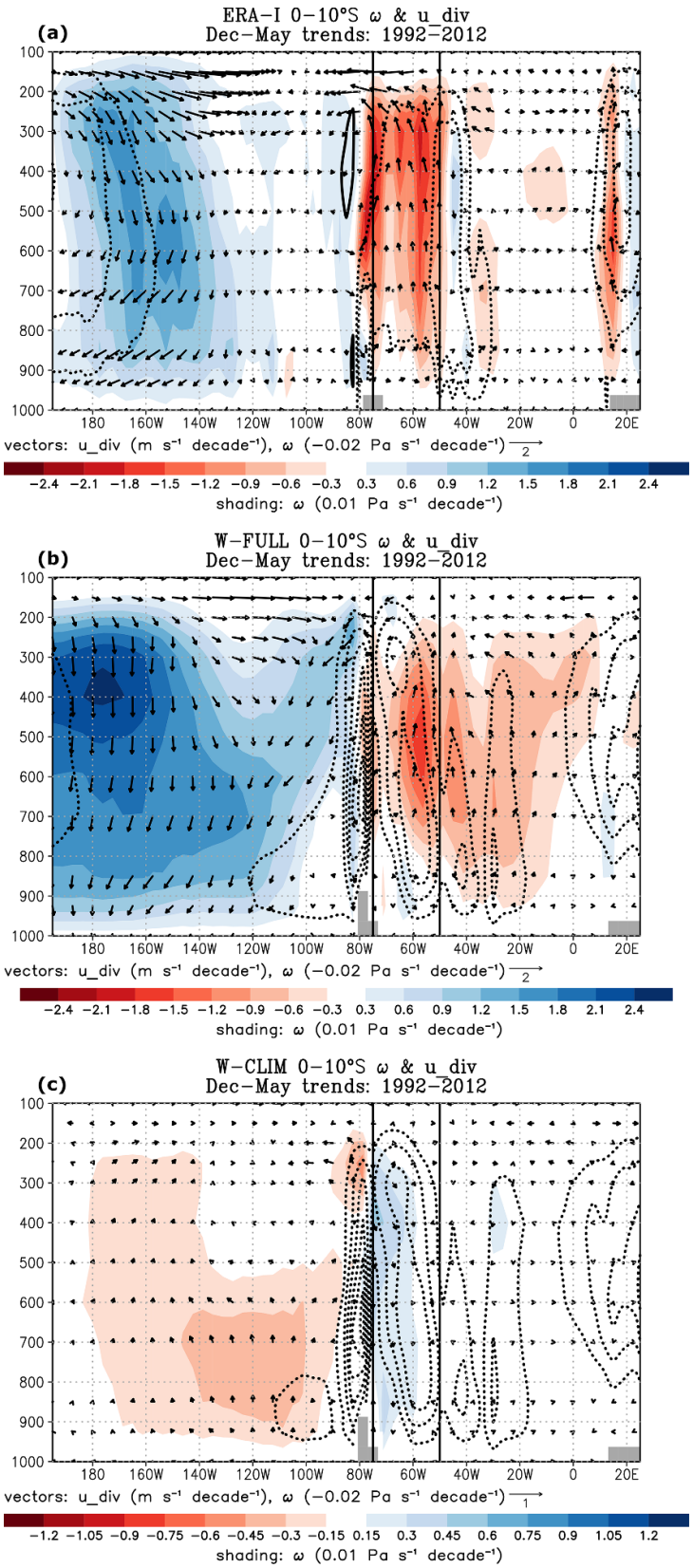

Figure 4. Equatorial atmospheric zonal circulation. 1992–2012 trends in December–May meridionally-averaged 0–10° S pressure vertical velocity (ω, in Pa s^{-1} decade^{-1}) and divergent zonal wind (u_{div}, in m s^{-1} decade^{-1}). Shading shows trends in ω, and vectors show trends in ω and u_{div}: (a) ERA-I, (b) W-FULL, and (c) W-CLIM (note doubled color and vector scales). The ω vector component is multiplied by a factor of −50. Contours show the 1980–1992 December–May mean ω climatology: solid contours show positive values, dashed contours show negative values; the contour interval is 0.02 Pa s^{-1}; and the zero contour is omitted. Vertical lines at 75° and 50° W outline the Amazon region.

these simulations are not directly comparable to our approach since they impose climatological SST outside the perturbed SST basin, whereas we allow ocean-atmosphere feedbacks through interactive air-sea coupling and include SST evolution from external forcings.

The W-CLIM setup assumes that tropical Pacific wind stress did not respond to external forcing during the observed strengthening period. This assumption has been challenged by findings that anthropogenic Asian sulfate aerosols contributed to the increased Pacific trade winds (Smith *et al* 2016, Takahashi and Watanabe 2016), though the linkage has been questioned (Oudar *et al* 2018). There is also evidence that the Pacific trade wind increase and Walker circulation strengthening were partly driven by teleconnections from Atlantic SST warming (McGregor *et al* 2014, Chikamoto *et al* 2015).

Interestingly, we find that W-CLIM high-season Amazon River discharge is significantly correlated with observations, though explaining only about half the variance as W-FULL (table 2). Examination of the Amazon River discharge time series reveals that much of the skill comes from decreases in 1983 and 1992 following the 1982 El Chichón and 1991 Mount Pinatubo eruptions (figure 2(e)), which is consistent with findings of reduced Amazon River discharge following large tropical eruptions (Iles and Hegerl 2015). The W-CLIM post-eruption decrease magnitudes are much smaller than in W-FULL, which incorporates Pacific trade wind anomalies related to the 1982–83 and 1991–92 El Niño events.

The Amazon region wet-season precipitation increase simulated in W-FULL is driven by increased moisture convergence via atmospheric dynamical changes, through a strengthened Walker circulation. However, within this large-scale framework, we note that the relatively low-resolution IPSL-CM5A-LR model does not directly simulate some of the convective-to-synoptic-scale features important for Amazon region wet-season precipitation, such as coastal-generated squall lines (Greco *et al* 1990, Garstang *et al* 1998). More work is needed to investigate the role of these higher-resolution processes over the Amazon Basin, for instance using dynamical downscaling (Ramos da Silva and Haas 2016).

Biases in IPSL-CM5A-LR may account for some of the spatial discrepancies between the observed and modeled changes over the Amazon Basin. The double ITCZ and excessive eastern Pacific cold tongue biases, common to many models (Li and Xie 2014, Zhang *et al* 2019), translate into too-weak southerly cross-equatorial winds (Hu and Fedorov 2018) and may explain the spurious moisture advection trend from the equatorial Pacific in W-FULL. Some circulation differences may also stem from the model's coarse orographic representation of the Andes Mountains (Insel *et al* 2010). Additional examination of *pacemaker*-type simulations such as those through the Decadal Climate Prediction Project (Boer *et al* 2016) can help assess the robustness of our results in a multi-model framework.

Insufficient tropical North Atlantic SST warming in our simulations may cause discrepancies in the equatorial Atlantic wind field and explain the lack of moisture advected by the model mean flow. The weak tropical North Atlantic warming may also account for W-FULL's lack of skill in simulating Amazon region dry season (July–October) precipitation and low-season river discharge (table S4 and figure S6), which are negatively associated with the tropical Atlantic interhemispheric SST contrast through the position of the ITCZ (Yoon and Zeng 2010, Fernandes *et al* 2015). The model could be missing the observed warming from declining North American and European sulfate aerosols (Cox *et al* 2008, Hua *et al* 2019), which do not vary in our simulations, or from increased ocean heat transport convergence to the tropical North Atlantic (Servain *et al* 2014).

Despite these caveats, our study provides strong evidence for the influence of the tropical Pacific on the intensification of Amazon Basin wet-season precipitation and high-season river discharge from the early 1990s to the early 2010s. As the Amazon region faces increasing anthropogenic stressors over the coming decades, understanding the role of decadal ocean-atmosphere variability will be important to reduce uncertainties in climate-related hydrological impacts. For instance, how might a continuation of the recent positive IPO phase since around 2013 (Meehl *et al* 2016, Cha *et al* 2018) affect Amazon Basin wet-season precipitation and high-season discharge given further tropical Atlantic warming? Additional comparative studies prescribing tropical Pacific wind stress could help in understanding the ongoing hydroclimate changes in the vital Amazon region.

Data availability statement

The data that support the findings of this study are available upon reasonable request from the authors.

Acknowledgments

A R F and M A B were supported by the UK NERC-funded SMURPHs project (NE/N006143/1). A R F, G G, and M K were also supported by the French ANR under the program Facing Societal, Climate and Environmental Changes (MORDICUS project, Grant ANR-13-SENV-0002). This work was granted access to the HPC resources of TGCC under the allocation 2015-017403 and 2016-017403 made by GENCI. GPCP was produced as part of the GEWEX effort under the WCRP. The ERSST and GPCP data were provided by the NOAA/OAR/ESRL PSL, and ERA-I was provided by ECMWF and C3S. The Amazon

discharge data at Óbidos were provided by the SO HYBAM Amazon Basin Water Resources Observation Service monitoring network (www.so-hybam.org). We appreciate the constructive feedback from three anonymous reviewers.

ORCID iDs

Andrew R Friedman https://orcid.org/0000-0001-6994-2037
Massimo A Bollasina https://orcid.org/0000-0001-7509-7650
Guillaume Gastineau https://orcid.org/0000-0002-5478-1119
Myriam Khodri https://orcid.org/0000-0003-1941-1646

References

Adler R F *et al* 2003 The version-2 global precipitation climatology project (GPCP) monthly precipitation analysis (1979–present) *J. Hydrometeorol.* **4** 1147–67
Adler R F *et al* 2018 The global precipitation climatology project (GPCP) monthly analysis (new version 2.3) and a review of 2017 global precipitation *Atmosphere* **9** 138
Andreoli R V, Souza R A F, De, Kayano M T and Candido L A 2012 Seasonal anomalous rainfall in the central and eastern Amazon and associated anomalous oceanic and atmospheric patterns *Int. J. Climatol.* **32** 1193–205
Angelini I M, Garstang M, Davis R E, Hayden B, Fitzjarrald D R, Legates D R, Greco S, Macko S and Connors V 2011 On the coupling between vegetation and the atmosphere *Theor. Appl. Climatol.* **105** 243–61
Arraut J M, Nobre C, Barbosa H M J, Obregon G and Marengo J 2012 Aerial rivers and lakes: looking at large-scale moisture transport and its relation to Amazonia and to subtropical rainfall in South America *J. Clim.* **25** 543–56
Balmaseda M A, Trenberth K E and Källén E 2013 Distinctive climate signals in reanalysis of global ocean heat content *Geophys. Res. Lett.* **40** 1754–9
Barichivich J, Gloor E, Peylin P, Brienen R J W, Schöngart J, Espinoza J C and Pattnayak K C 2018 Recent intensification of Amazon flooding extremes driven by strengthened Walker circulation *Sci. Adv.* **4** eaat8785
Bellenger H, Guilyardi É, Leloup J, Lengaigne M and Vialard J 2014 ENSO representation in climate models: from CMIP3 to CMIP5 *Clim. Dyn.* **42** 1999–2018
Boer G J *et al* 2016 The decadal climate prediction project (DCPP) contribution to CMIP6 *Geosci. Model Dev.* **9** 3751–77
Bretherton C S, Widmann M, Dymnikov V P, Wallace J M and Bladé I 1999 The effective number of spatial degrees of freedom of a time-varying field *J. Clim.* **12** 1990–2009
Cha S-C, Moon J-H and Song Y T 2018 A recent shift toward an El Niño-like ocean state in the tropical Pacific and the resumption of ocean warming *Geophys. Res. Lett.* **45** 11885–94
Chikamoto Y, Timmermann A, Luo J-J, Mochizuki T, Kimoto M, Watanabe M, Ishii M, Xie S-P and Jin F-F 2015 Skilful multi-year predictions of tropical trans-basin climate variability *Nat. Commun.* **6** 6869
Clarke A J 2008 *Introduction to the Dynamics of El Niño and the Southern Oscillation* (New York: Academic)
Cox P M, Harris P P, Huntingford C, Betts R A, Collins M, Jones C D, Jupp T E, Marengo J A and Nobre C A 2008 Increasing risk of Amazonian drought due to decreasing aerosol pollution *Nature* **453** 212–5
Dai A 2016 Historical and future changes in streamflow and continental runoff *Terrestrial Water Cycle and Climate Change: Natural and Human-Induced Impacts* (*Geophysical Monograph Series*) (Washington, DC: American Geophysical Union) pp 17–37
Dai A, Qian T, Trenberth K E and Milliman J D 2009 Changes in continental freshwater discharge from 1948 to 2004 *J. Clim.* **22** 2773–92
Dai A and Trenberth K E 2002 Estimates of freshwater discharge from continents: latitudinal and seasonal variations *J. Hydrometeorol.* **3** 660–87
Dai A and Wigley T M L 2000 Global patterns of ENSO-induced precipitation *Geophys. Res. Lett.* **27** 1283–6
de Boisséson E, Balmaseda M A, Abdalla S, Källén E and Janssen P A E M 2014 How robust is the recent strengthening of the Tropical Pacific trade winds? *Geophys. Res. Lett.* **41** 4398–405
Dee D P *et al* 2011 The ERA-Interim reanalysis: configuration and performance of the data assimilation system *Q. J. R. Meteorol. Soc.* **137** 553–97
Dinezio P N, Clement A C, Vecchi G A, Soden B J, Kirtman B P and Lee S-K 2009 Climate response of the equatorial Pacific to global warming *J. Clim.* **22** 4873–92
Dong B and Lu R 2013 Interdecadal enhancement of the walker circulation over the Tropical Pacific in the late 1990s *Adv. Atmos. Sci.* **30** 247–62
Douville H, Voldoire A and Geoffroy O 2015 The recent global warming hiatus: what is the role of Pacific variability? *Geophys. Res. Lett.* **42** 2014GL062775
Drumond A, Marengo J, Ambrizzi T, Nieto R, Moreira L and Gimeno L 2014 The role of the Amazon Basin moisture in the atmospheric branch of the hydrological cycle: a Lagrangian analysis *Hydrol. Earth Syst. Sci.* **18** 2577–98
Dufresne J-L *et al* 2013 Climate change projections using the IPSL-CM5 Earth system model: from CMIP3 to CMIP5 *Clim. Dyn.* **40** 2123–65
England M H, McGregor S, Spence P, Meehl G A, Timmermann A, Cai W, Gupta A S, Mcphaden M J, Purich A and Santoso A 2014 Recent intensification of wind-driven circulation in the Pacific and the ongoing warming hiatus *Nat. Clim. Change* **4** 222–7
Fernandes K, Giannini A, Verchot L, Baethgen W and Pinedo-Vasquez M 2015 Decadal covariability of Atlantic SSTs and western Amazon dry-season hydroclimate in observations and CMIP5 simulations *Geophys. Res. Lett.* **42** 6793–801
Foley J A, Botta A, Coe M T and Costa M H 2002 El Niño–Southern oscillation and the climate, ecosystems and rivers of Amazonia *Glob. Biogeochem. Cycles* **16** 79-1–20
Frankignoul C, Gastineau G and Kwon Y-O 2017 Estimation of the SST response to anthropogenic and external forcing and its impact on the Atlantic Multidecadal Oscillation and the Pacific Decadal Oscillation *J. Clim.* **30** 9871–95
Garstang M, White S, Shugart H H and Halverson J 1998 Convective cloud downdrafts as the cause of large blowdowns in the Amazon rainforest *Meteorol. Atmos. Phys.* **67** 199–212
Gastineau G, Friedman A R, Khodri M and Vialard J 2019 Global ocean heat content redistribution during the 1998–2012 Interdecadal Pacific oscillation negative phase *Clim. Dyn.* **53** 1187–208
Gastineau G, Friedman A R, Khodri M and Vialard J 2020 Correction to: global ocean heat content redistribution during the 1998–2012 Interdecadal Pacific oscillation negative phase *Clim. Dyn.* **55** 2311
Gloor M, Barichivich J, Ziv G, Brienen R, Schöngart J, Peylin P, Cintra B B L, Feldpausch T, Phillips O and Baker J 2015 Recent Amazon climate as background for possible ongoing and future changes of Amazon humid forests *Glob. Biogeochem. Cycles* **29** 1384–99
Gloor M, Brienen R J W, Galbraith D, Feldpausch T R, Schöngart J, Guyot J-L, Espinoza J C, Lloyd J and Phillips O L 2013

Intensification of the Amazon hydrological cycle over the last two decades *Geophys. Res. Lett.* **40** 1729–33
Gouveia N A, Gherardi D F M and Aragão L E O C 2019 The role of the Amazon River plume on the intensification of the hydrological cycle *Geophys. Res. Lett.* **46** 122219
Greco S, Swap R, Garstang M, Ulanski S, Shipham M, Harriss R C, Talbot R, Andreae M O and Artaxo P 1990 Rainfall and surface kinematic conditions over central Amazonia during ABLE 2B *J. Geophys. Res. Atmos.* **95** 17001–14
Grimm A M 2003 The El Niño impact on the summer monsoon in Brazil: regional processes versus remote influences *J. Clim.* **16** 263–80
Guimberteau M *et al* 2012 Discharge simulation in the sub-Basins of the Amazon using ORCHIDEE forced by new datasets *Hydrol. Earth Syst. Sci.* **16** 911–35
Guimberteau M, Ducharne A, Ciais P, Boisier J P, Peng S, De Weirdt M and Verbeeck H 2014 Testing conceptual and physically based soil hydrology schemes against observations for the Amazon Basin *Geosci. Model Dev.* **7** 1115–36
Hegerl G and Zwiers F 2011 Use of models in detection and attribution of climate change *Wiley Interdiscip. Rev. Clim. Change* **2** 570–91
Hourdin F *et al* 2013 Impact of the LMDZ atmospheric grid configuration on the climate and sensitivity of the IPSL-CM5A coupled model *Clim. Dyn.* **40** 2167–92
Hu S and Fedorov A V 2018 Cross-equatorial winds control El Niño diversity and change *Nat. Clim. Change* **8** 798–802
Hua W, Dai A, Zhou L, Qin M and Chen H 2019 An externally forced decadal rainfall seesaw pattern over the Sahel and Southeast Amazon *Geophys. Res. Lett.* **46** 923–32
Huang B, Thorne P W, Banzon V F, Boyer T, Chepurin G, Lawrimore J H, Menne M J, Smith T M, Vose R S and Zhang H-M 2017 NOAA extended reconstructed sea surface temperature (ERSST), version 5 (https://doi.org/10.7289/V5T72FNM)
Huang P 2014 Regional response of annual-mean tropical rainfall to global warming *Atmos. Sci. Lett.* **15** 103–9
Iles C E and Hegerl G C 2015 Systematic change in global patterns of streamflow following volcanic eruptions *Nat. Geosci.* **8** 838
Insel N, Poulsen C J and Ehlers T A 2010 Influence of the Andes Mountains on South American moisture transport, convection, and precipitation *Clim. Dyn.* **35** 1477–92
Jahfer S, Vinayachandran P N and Nanjundiah R S 2017 Long-term impact of Amazon river runoff on northern hemispheric climate *Sci. Rep.* **7** 10989
Jones C and Carvalho L M V 2013 Climate change in the South American Monsoon system: present climate and CMIP5 projections *J. Clim.* **26** 6660–78
Kerr R A 2000 A North Atlantic climate pacemaker for the centuries *Science* **288** 1984–5
Khodri M *et al* 2017 Tropical explosive volcanic eruptions can trigger El Niño by cooling tropical Africa *Nat. Commun.* **8** 778
Kosaka Y and Xie S-P 2013 Recent global-warming hiatus tied to equatorial Pacific surface cooling *Nature* **501** 403–7
Krinner G, Viovy N, de Noblet-ducoudré N, Ogée J, Polcher J, Friedlingstein P, Ciais P, Sitch S and Prentice I C 2005 A dynamic global vegetation model for studies of the coupled atmosphere-biosphere system *Glob. Biogeochem. Cycles* **19** GB1015
Li G and Xie S-P 2014 Tropical biases in CMIP5 multimodel ensemble: the excessive equatorial Pacific cold tongue and double ITCZ problems *J. Clim.* **27** 1765–80
Liu B and Zhou T 2017 Atmospheric footprint of the recent warming slowdown *Sci. Rep.* **7** 40947
Ma J and Xie S-P 2013 Regional patterns of sea surface temperature change: a source of uncertainty in future projections of precipitation and atmospheric circulation *J. Clim.* **26** 2482–501
Madec G 2008 NEMO ocean engine (available at: http://nora.nerc.ac.uk/164324/) (Accessed 12 April 2016)
Malhi Y, Roberts J, Betts R, Killeen T, Li W and Nobre C 2008 Climate change, deforestation, and the fate of the Amazon *Science* **319** 169–72
Marengo J A 2005 Characteristics and spatio-temporal variability of the Amazon River Basin water budget *Clim. Dyn.* **24** 11–22
Marengo J A *et al* 2012 Recent developments on the South American monsoon system *Int. J. Climatol.* **32** 1–21
Marengo J A and Espinoza J C 2016 Extreme seasonal droughts and floods in Amazonia: causes, trends and impacts *Int. J. Climatol.* **36** 1033–50
Marengo J A, Souza C M J, Thonicke K, Burton C, Halladay K, Betts R A, Alves L M and Soares W R 2018 Changes in climate and land use over the Amazon Region: current and future variability and trends *Front. Earth Sci.* **6** 228
McGregor S, Timmermann A, Stuecker M F, England M H, Merrifield M, Jin F-F and Chikamoto Y 2014 Recent Walker circulation strengthening and Pacific cooling amplified by Atlantic warming *Nat. Clim. Change* **4** 888–92
Meehl G A, Arblaster J M, Fasullo J T, Hu A and Trenberth K E 2011 Model-based evidence of deep-ocean heat uptake during surface-temperature hiatus periods *Nat. Clim. Change* **1** 360–4
Meehl G A, Hu A and Teng H 2016 Initialized decadal prediction for transition to positive phase of the Interdecadal Pacific oscillation *Nat. Commun.* **7** 1–7
Molinier M, Guyot J-L, de Oliveira E and Guimaraes V 1996 Les régimes hydrologiques de l'Amazone et de ses affluents *L'hydrologie Tropicale : Géosciences Et Outil Pour Le Développement: Mélanges À La Mémoire De Jean Rodier, Publication—AISH* ed P Chevallier and B Pouyaud (Wallingford: AISH) pp 209–22
Nobre C A, Sampaio G, Borma L S, Castilla-Rubio J C, Silva J S and Cardoso M 2016 Land-use and climate change risks in the Amazon and the need of a novel sustainable development paradigm *Proc. Natl Acad. Sci.* **113** 10759–68
Oudar T, Kushner P J, Fyfe J C and Sigmond M 2018 No impact of anthropogenic aerosols on early 21st century global temperature trends in a large initial-condition ensemble *Geophys. Res. Lett.* **45** 9245–52
Power S, Casey T, Folland C, Colman A and Mehta V 1999 Inter-decadal modulation of the impact of ENSO on Australia *Clim. Dyn.* **15** 319–24
Ramos da Silva R and Haas R 2016 Ocean global warming impacts on the South America climate *Front. Earth Sci.* **4** 30
Ropelewski C F and Halpert M S 1987 Global and regional scale precipitation patterns associated with the El Niño/Southern oscillation *Mon. Weather Rev.* **115** 1606–26
Santer B D, Wigley T M L, Boyle J S, Gaffen D J, Hnilo J J, Nychka D, Parker D E and Taylor K E 2000 Statistical significance of trends and trend differences in layer-average atmospheric temperature time series *J. Geophys. Res. Atmos.* **105** 7337–56
Satyamurty P, da Costa C P W and Manzi A O 2013a Moisture source for the Amazon Basin: a study of contrasting years *Theor. Appl. Climatol.* **111** 195–209
Satyamurty P, da Costa C P W, Manzi A O and Candido L A 2013b A quick look at the 2012 record flood in the Amazon Basin *Geophys. Res. Lett.* **40** 1396–401
Servain J, Caniaux G, Kouadio Y K, Mcphaden M J and Araujo M 2014 Recent climatic trends in the tropical Atlantic *Clim. Dyn.* **43** 3071–89
Smith D M, Booth B B B, Dunstone N J, Eade R, Hermanson L, Jones G S, Scaife A A, Sheen K L and Thompson V 2016 Role of volcanic and anthropogenic aerosols in the recent global surface warming slowdown *Nat. Clim. Change* **6** 936
Takahashi C and Watanabe M 2016 Pacific trade winds accelerated by aerosol forcing over the past two decades *Nat. Clim. Change* **6** 768–72
Taylor K E, Stouffer R J and Meehl G A 2012 An overview of CMIP5 and the experiment design *Bull. Am. Meteorol. Soc.* **93** 485–98
Vecchi G A and Soden B J 2007 Global warming and the weakening of the tropical circulation *J. Clim.* **20** 4316–40

Wang C 2006 An overlooked feature of tropical climate: inter-Pacific-Atlantic variability *Geophys. Res. Lett.* **33** L12702

Wang X-Y, Li X, Zhu J and Tanajura C A S 2018 The strengthening of Amazonian precipitation during the wet season driven by tropical sea surface temperature forcing *Environ. Res. Lett.* **13** 094015

Watanabe M, Shiogama H, Tatebe H, Hayashi M, Ishii M and Kimoto M 2014 Contribution of natural decadal variability to global warming acceleration and hiatus *Nat. Clim. Change* **4** 893

Yin L, Fu R, Shevliakova E and Dickinson R E 2013 How well can CMIP5 simulate precipitation and its controlling processes over tropical South America? *Clim. Dyn.* **41** 3127–43

Yoon J-H and Zeng N 2010 An Atlantic influence on Amazon rainfall *Clim. Dyn.* **34** 249–64

Zhang G J, Song X and Wang Y 2019 The double ITCZ syndrome in GCMs: a coupled feedback problem among convection, clouds, atmospheric and ocean circulations *Atmos. Res.* **229** 255–68

Zhang Y, Wallace J M and Battisti D S 1997 ENSO-like interdecadal variability: 1900–93 *J. Clim.* **10** 1004–20